Chevalier, Thibaud; Koivisto, Juha; Shmakova, N.; Alava, Mikko; Puisto, Antti; Raufaste, C.;
Santucci, Stephane

Foam flows through a local constriction

Foam flows through a local constriction

Related content

Foam flows through a local constriction

T Chevalier[1], J Koivisto[1], N Shmakova[2], M J Alava[1], A Puisto[1], C Raufaste[3] and S Santucci [2, 4]

[1] COMP Center of Excellence, Department of Applied Physics, Aalto University, Espoo, Finland
[2] Lavrentyev Institute of Hydrodynamics SB RAS, Novosibirsk, Russia
[3] Université Côte d'Azur, CNRS, Institut de Physique de Nice, 06100 Nice, France
[4] Laboratoire de Physique, ENS de Lyon, Univ Lyon, CNRS, UMR 5672, Lyon, France

E-mail: stephane.santucci@ens-lyon.fr

Abstract. We present an experimental study of the flow of a liquid foam, composed of a monolayer of millimetric bubbles, forced to invade an inhomogeneous medium at a constant flow rate. To model the simplest heterogeneous fracture medium, we use a Hele-Shaw cell consisting of two glass plates separated by a millimetric gap, with a local constriction. This single defect localized in the middle of the cell reduces locally its gap thickness, and thus its local permeability. We investigate here the influence of the geometrical property of the defect, specifically its height, on the average steady-state flow of the foam. In the frame of the flowing foam, we can observe a clear recirculation around the obstacle, characterized by a quadrupolar velocity field with a negative wake downstream the obstacle, which intensity evolves systematically with the obstacle height.

1. Introduction

Liquid foams, such as chocolate mousse and shaving foams are soft materials that we all use in our everyday life. Their multi-scale biphasic structure of gas bubbles within a liquid phase leads to a dual mechanical behaviour: they behave as solids at rest, while they can flow like liquids above a given critical yield stress. Such peculiar rheological properties are at the root of their use in diverse applications, ranging from daily-life products developed in food, cosmetics and pharmaceutical industries, to larger scale industrial processes, for instance in oil recovery or soil remediation. For those last applications, understanding and controlling the flow of liquid foams in confined heterogeneous media appears of tremendous importance [1][2][3][4].

Thus, in order to investigate the flow of liquid foams and more specifically, the motion, deformation and topological rearrangements of the bubbles, when forced to invade a heterogeneous porous and fractured medium, we have designed the following simple experimental set-up.

2. Experimental set-up

2.1. A simple model fracture

Our set-up allows the direct observation of the motion and deformation of the elementary components of a 2D liquid foam, the bubbles, when forced to invade a confined medium that mimics a simple model fracture. As shown on figure 1, our model fracture consists of an inhomogeneous Hele-Shaw cell, made of 2 glass plates (15 cm wide, 50 cm long and 1 cm thick), separated by a 1 mm gap. Moreover, the cell can present a defect of lateral size 2 x 2 cm2 and height H of typically a few hundred of microns. This bump localized in the centre of the cell reduces locally its gap, and thus decreases locally the permeability of the cell. To ensure identical surface properties of the top and bottom plates of the cell, both surfaces are covered with a thin stretchable hydrophilic plastic film, leading to a trapezoidal shape of the constriction, as shown on the side view of the cell displayed in figure 1, (panel a).

2.2. In-situ generation & forced flow of a liquid foam

We generate in-situ our liquid foam and forced it to flow at a constant velocity in our model fracture, by bubbling filtered pressurized air, at a constant rate of 40 ml/mn (thanks to a mass flow controller) through a needle of inner diameter 0.45 mm, in a vertical chamber connected to the cell (via a 10 mm diameter hole drilled in the bottom plate), filled with a soapy solution. This surfactant solution is obtained by mixing 1% of a commercial dishwashing liquid Dawn© with ultra-pure water.

In these conditions, the bubbles generated are quasi mono-disperse with a diameter larger than the cell gap. Therefore, those bubbles form a 2D confined foam, constituted by a mono-layer of millimetric bubbles. It is also important to notice that those experimental conditions lead to a constant flow rate of the liquid foam, invading the inhomogeneous cell at a velocity around v = 15 mm/s.
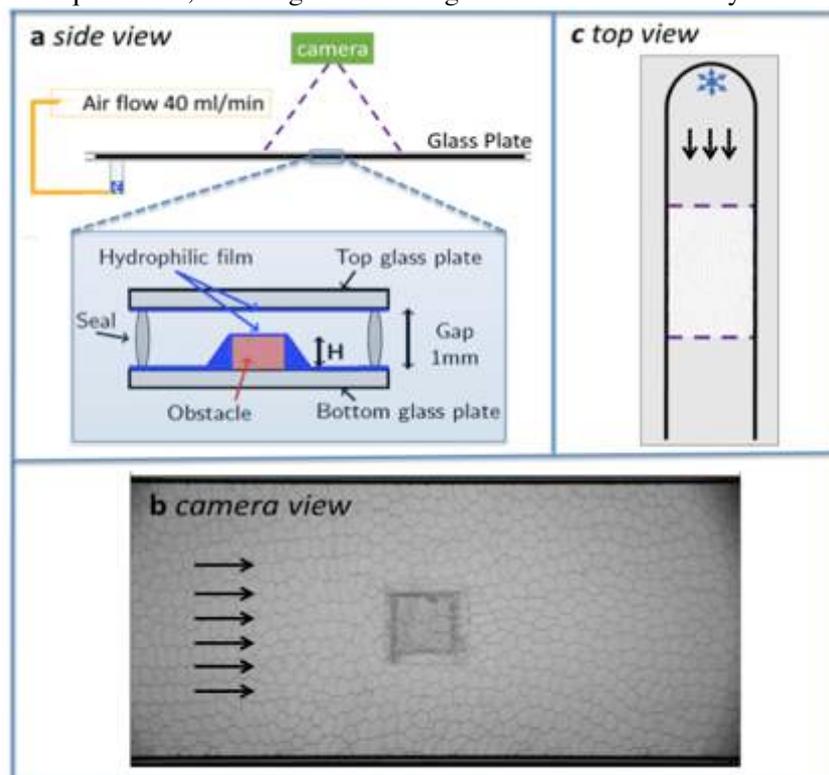
Figure 1: Experimental set-up, allowing the direct observation of a 2D liquid foam flowing in a Hele-Shaw cell with a local constriction, due to an obstacle placed in the middle of the cell (the obstacle height H is smaller than the gap of the cell, G =1 mm). The panels (a) and (c) displays respectively side and top views, while the bottom panel shows a typical recorded image (b), for a flow experiment with an obstacle filling 70% of the gap cell.

2.3. Direct observation

We observe directly the steady-state flow of our 2D liquid foam in the middle of the cell around the obstacle with an imaging area of 20 x 10 cm, using a Ximea XiQ digital camera during 400 seconds at 5 Hz. Thus, we record 2000 frames with a resolution of 2088 x 1048 pixels. A typical image recorded during a flow experiment with an obstacle filling 70% of the gap cell is shown on the bottom panel of figure 1, as well as a zoom in a region around the obstacle on the left panel of figure 2.

3. Image analysis

Using standard image analysis tools, developed within the software ImageJ© and MATLAB©, we can obtain a network of skeletonized bubbles (a zoom around the obstacle of a typical binary image of the bubble network obtained by edge detection is shown on the right panel of figure 2). We can subsequently identify all individual bubbles of the flowing foam, for each recorded image.

Interestingly, one can already observe that the bubbles approaching the constriction get squeezed in the direction of the imposed mean flow, while the bubbles exiting the permeable defect are strongly elongated in this direction. Moreover, the bubbles on the obstacle have an apparent increase of diameter obviously related to the reduction of the gap cell thickness and their incompressible nature.
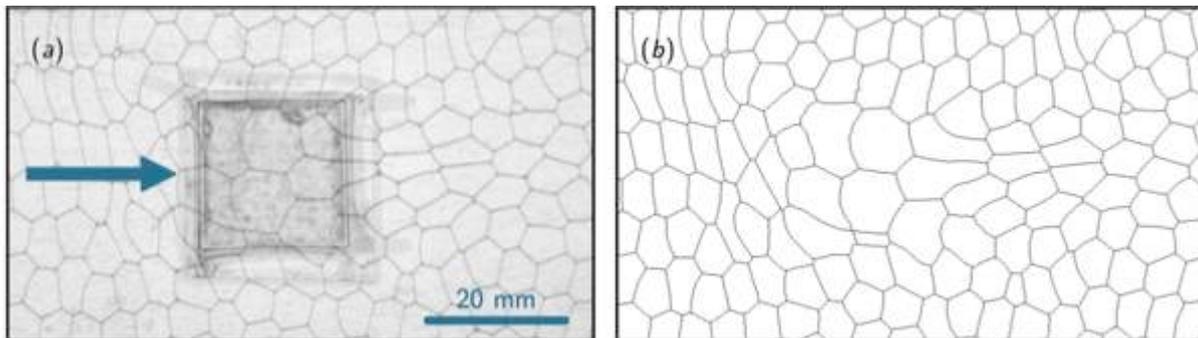

Figure 2: The left panel (a) shows a zoom (on a region around the obstacle) of a raw image recorded by the camera during the foam flow with an obstacle filling 70% of the gap cell. The arrow shows the direction of the imposed flow. The right panel (b) displays the corresponding binary image of the skeletonized bubble network obtained by edge detection, over the same region. The shaded square zone gives the location of the constriction.

4. Averaged velocity field

Tracking those labelled bubbles, we can measure their velocity by computing the displacement vector of the bubble centres, between two subsequent images recorded with a time delay of $\Delta t = 0.2$ s. The resulting average velocity field for an experiment with an obstacle filling 70% of the gap cell is shown in figure 3.

Furthermore, we have checked that the velocity field of the flowing foam could also be obtained by standard image correlation techniques, using directly the texture provided by the films of the bubbles themselves and their vertices. To perform this task, we took advantage of PIVlab – a Time-Resolved Digital Particle Image Velocimetry Toolbox for MATLAB – developed by W. Thielicke and E. J. Stamhuis to compute the velocity fields shown in figure 4[5]. Furthermore, we could obtain similar velocity fields using solely the vertices of the skeletonized bubble network as tracers of the flow. Such a result appears particularly interesting. Indeed, the same procedure could be extrapolated in 3D to extract easily the velocity field of a 3D liquid foam flowing in a constriction or around an obstacle, such as the one captured recently using ultra fast X-ray tomography [6], without the need of the very tedious and still unclear procedure of the reconstruction of the 3D bubbles shape [7].
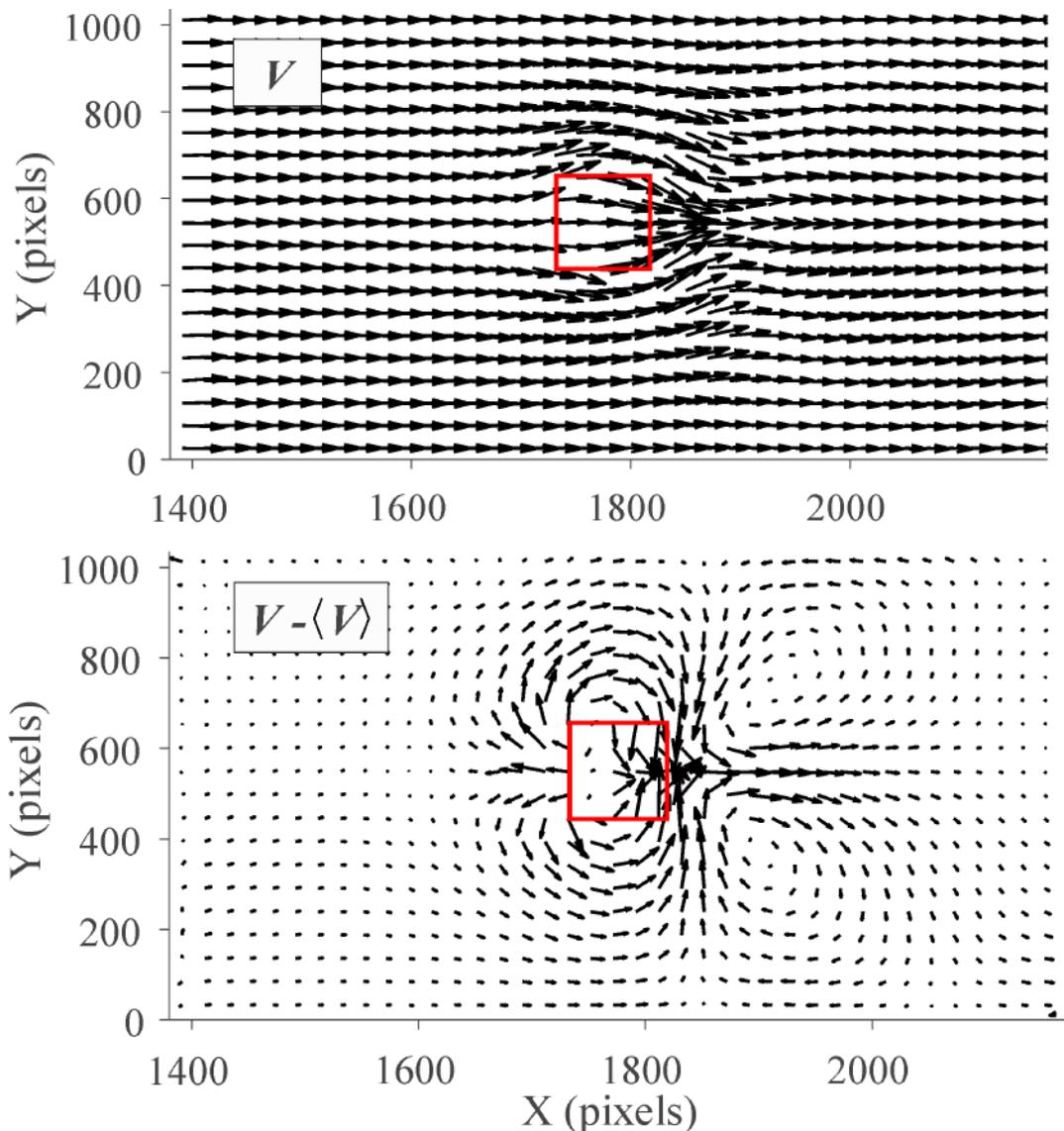
Figure 3: Average velocity field (obtained by tracking bubble centers) for a flow experiment with an obstacle (red square of 2x2 cm^2) filling 70 % of the cell gap. On the bottom panel, the imposed flow rate at the inlet is substracted to the velocity field, revealing the strong disturbance induced by the constriction characterized by a quadrupolar velocity field around the obstacle and an ovsershoot downstream the obstacle.

Far from the constriction, we clearly observe that the velocity field is uniform corresponding to the flow rate imposed by our experimental procedure. Nevertheless, approaching the permeable obstacle, the amplitude of the velocity field decreases, while it increases when leaving the obstacle. Such flow disturbance caused by the constriction is clearly revealed when displaying the velocity field in the frame of the flowing foam (shown in the bottom panel of figure 3, as well as in figure 4). Indeed, a clear recirculation is then observed, characterized by a quadrupolar velocity field around the obstacle. Furthermore, downstream the obstacle, there is a zone where the velocity is larger than the mean velocity (equivalently, in the frame of the flowing foam, the velocity is opposed to the one of the obstacle). Such effect is reminiscent of the observation of a so-called "negative wake" in the flow pattern of rising air bubbles in viscoelastic fluids [8].
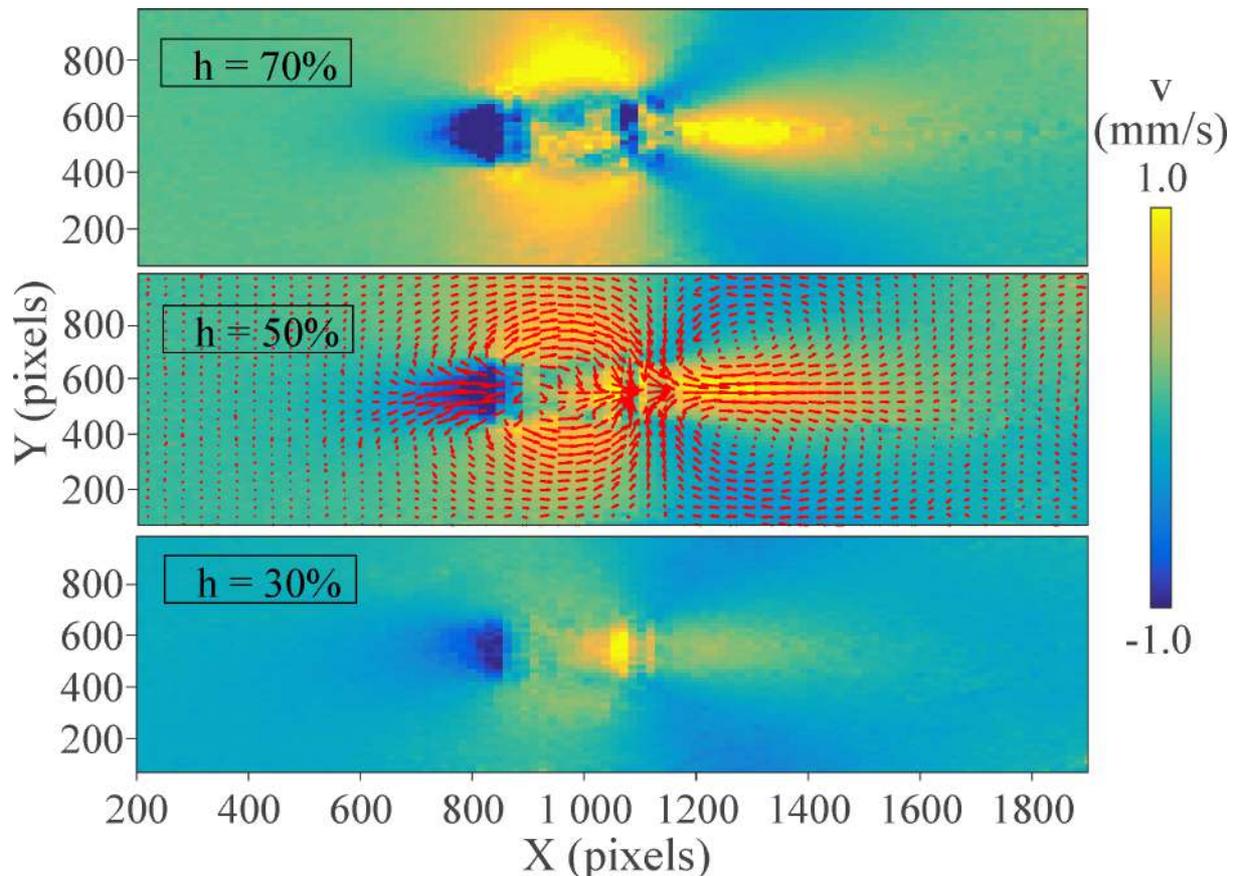
Figure 4: Velocity field (obtained by image correlation – using PIVLAB) averaged over 100 susbequent frames, corresponding to monitoring the liquid foam flow for 20 s. The different panels correspond to flow experiments for different heights of the obstacle, filling respectively 70%, 50% and 30% the gap cell. A flow rate of 15 mm/s imposed at the inlet is substracted to the velocity field in order to reveal the recirculation around the obstacle.

Our observations and results appear analogous to the ones obtained for a 2-D foam flow around a full obstacle (using a liquid pool geometry), characterized in detail by Dollet and Graner [3], Raufaste et al [6], which were attributed to the visco-elasto-plastic nature of the foam [10], that cannot be modelled as a simple visco-plastic fluid.

Interestingly, in our geometry, modifying locally the permeability of the cell (by simply changing the height of the defect/constriction), we can modulate systematically the intensity of the quadrupolar recirculation and specifically the velocity overshoot observed behind the obstacle. Figure 4 shows clearly that while such quadrupolar velocity field is already present for a very mild variation of the gap cell, locally, the amplitude of the disturbance and specifically the intensity of the recirculation increases systematically with the height of the local permeable obstacle.

5. Conclusions and perspectives

We have designed a simple but original experimental set-up to directly observe the motion and deformation of the bubbles of a 2D liquid foam, forced to invade an inhomogeneous confined medium at a constant flow rate. We could show that a constriction (reducing locally the gap of the cell) modifies strongly the average steady–state flow of the foam, leading to a quadrupolar velocity field in the frame of the flowing foam around this permeable obstacle. The intensity of such recirculation (and in particular the velocity overshoot observed downstream the constriction) increases systematically with the constriction height.

Following the procedure and tools developed by Dollet and Graner [3], Raufaste et al [9], Marmottant et al [11], we are currently investigating in detail the influence of the geometrical properties of the localized constriction (shape, lateral extension and height of the permeable defect), as well as other experimental controlling parameters, such as the foam liquid fraction and the imposed flow rate on both the velocity, deformation and the topological rearrangement of the bubbles. On the other hand, we are also implementing the so-called "Bubble model" [12] within our specific geometry in order to check if such simple model is able to reproduce the foam flow observed experimentally.

Acknowledgements

References

[1]   Weaire D and Hutzler S 1999 *The Physics of Foams* (Oxford University Press)
[2]   Cantat I, Cohen-Addad S, Elias F, Graner F, Hohler R, Pitois O, Rouyer F and Saint-Jalmes A 2013 *Foams, Structure and Dynamics* (Oxford University Press)
[3]   Dollet B and Graner F 2007 Two-dimensional flow of foam around a circular obstacle: Local measurements of elasticity, plasticity and flow *J. Fluid Mech.* **585** 181
[4]   Stevenson P 2012 *Foam Engineering: Fundamentals and Applications* (Wiley)
[5]   Thielicke W and Stamhuis E J 2014 PIVlab – Towards User-friendly, Affordable and Accurate Digital Particle Image Velocimetry in MATLAB *Journal of Open Research Software* **2**
[6]   Raufaste C, Dollet B, Santucci S and Mokso R 2015 Three-dimensional foam flow resolved by fast X-ray tomographic microscopy *EPL* **111** 38004
[7]   Mader K, Mokso R, Raufaste C, Dollet B, Santucci S, Lambert J, Stampanoni M 2012 Quantitative 3D Characterization of Cellular Materials: Segmentation and Morphology of Foam *Colloids Surf. A* **415** 230
[8]   Hassager O 1979 Negative wake behind bubbles in non-newtonian fluids *Nature* **279** 402
[9]   Raufaste C, Dollet B, Cox S, Jiang Y and Graner F 2007 Yield drag in a two-dimensional foam flow around a circular obstacle: Effect of liquid fraction *Eur. Phys. J. E* **23** 217
[10]   Cheddadi I, Saramito P, Dollet B, Raufaste C, Graner F 2011 Understanding and predicting viscous, elastic, plastic flows *Eur. Phys. J. E* **34** 1
[11]   Marmottant P, Raufaste C and Graner F 2008 Discrete rearranging disordered patterns Part II: D plasticity, elasticity and flow of a foam *Eur. Phys. J. E* **25** 371
[12]   Durian D J 1995 Foam Mechanics at the Bubble Scale *Phys. Rev. Lett.* **75** 4780